JOURNAL OF BACTERIOLOGY, July 1996, p. 4012–4019 Vol. 178, No. 14
0021-9193/96/$04.00+0


# Transcript Analysis of the c-*vac* Region and Differential Synthesis of the Two Regulatory Gas Vesicle Proteins GvpD and GvpE in *Halobacterium salinarium* PHH4

KERSTIN KRÜGER AND FELICITAS PFEIFER*

*Institut für Mikrobiologie und Genetik, Technische Hochschule Darmstadt, D-64287 Darmstadt, Germany*

Received 5 March 1996/Accepted 1 May 1996

***Halobacterium salinarium*** **PHH4 synthesizes gas vesicles in the stationary growth phase by the expression of 14 *gvp* genes arranged in two clusters. The chromosomal *gvpACNO* (c-*gvpACNO*) gene cluster (encoding the major structural gas vesicle protein GvpA and the minor structural protein GvpC) was transcribed as three mRNA species starting at one promoter during the stationary phase of growth. The second gene cluster, c-*gvpDEFGHIJKLM*, was transcribed during all stages of growth as a relatively unstable, single mRNA with a maximal length of 6 kb. In addition, a 1.7-kb c-*gvpD* transcript was synthesized during stationary growth starting at the same promotor as that of the c-*gvpDEFGHIJKLM* mRNA. The expression of the first two genes located in this unit (c-*gvpD* and c-*gvpE*) was also monitored by Western blot (immunoblot) analyses using antisera raised against these proteins synthesized in *Escherichia coli*. While the cGvpD protein was present only during early exponential growth and disappeared during gas vesicle formation, the cGvpE protein was present during cGvpA and gas vesicle synthesis in the early stationary phase of growth. Previous data indicated that cGvpD is involved in repression of gas vesicle formation, whereas cGvpE is a transcriptional activator for the c-*gvpA* promoter. The appearance of both proteins during the growth cycle is in line with the functions of these proteins in gas vesicle synthesis. The mechanism of the differential translation of cGvpD and cGvpE from the c-*gvpDEFGHIJKLM* mRNA still has to be elucidated, but antisense RNAs complementary to the 5′ terminus as well as the 3′ portion of the c-*gvpD* mRNA might be involved in this regulation. Such RNAs occurred during early stationary growth when the cGvpD protein level decreased and may possibly inhibit the translation of the c-*gvpD* mRNA.**

Various aquatic bacteria as well as halophilic archaea possess gas vesicles conferring buoyancy to the cell and enabling them to float to the surfaces of their watery environments. Gas vesicles are proteinaceous structures filled with gas by passive diffusion (for a review, see reference 31). Among halophilic archaea, *Halobacterium salinarium*, *Haloferax mediterranei*, and *Natronobacterium vacuolatum* synthesize gas vesicles (7, 15, 18, 27).

The 14 genes involved in gas vesicle (Vac) synthesis of *H. salinarium* and *Haloferax mediterranei* are clustered in a genomic region termed the *vac* region. Different *vac* regions which are located either on endogenous plasmids (p-*vac*) (such as the 150-kb plasmid pHH1 of *H. salinarium* PHH1 and the plasmid pNRC100 of *H. salinarium* NRC-1) or on the chromosome (c-*vac* for the second *vac* region in *H. salinarium* PHH1 or mc-*vac* for the *vac* region in *Haloferax mediterranei*) have been characterized (5, 8, 14, 16). The wild-type strain *H. salinarium* PHH1 contains the two *vac* regions p-*vac* and c-*vac*, but only the p-*vac* region is expressed and leads to the synthesis of spindle-shaped gas vesicles throughout the growth cycle. The c-*vac* region is expressed only when the p-*vac* region is deleted, as has been found for *H. salinarium* PHH4 carrying plasmid pHH4, which is a 35-kb deletion variant of plasmid pHH1 (15, 21). In contrast to the spindle-shaped gas vesicles of wild-type *H. salinarium* PHH1, c-*vac*-encoded gas vesicles are cylindrical and appear only in the stationary growth phase. *H. salinarium* NRC-1 exhibits a gas vesicle phenotype similar to that of *H. salinarium* PHH1, and the *vac* region found on plasmid pNRC100 is almost identical to the p-*vac* region (12, 16, 22).

The gas vesicle protein-encoding genes (*gvp*) of each *vac* region are arranged in two clusters: *gvpACNO* and, oriented in the opposite direction, *gvpDEFGHIJKLM* (8, 12). The requirement of p-*gvpO* for gas vesicle synthesis was under debate (4), but deletion of this gene results in gas vesicle-negative transformants, indicating that p-*gvpO* is essential for gas vesicle production (20). The genes *gvpA* and *gvpC* encode the gas vesicle structural proteins; the 8-kDa GvpA protein forms the ribs of the gas vesicle wall, and the more hydrophilic 20-kDa GvpC protein is possibly located on the outside of the wall, tightening the overall gas vesicle structure as in the case of cyanobacterial gas vesicles (9, 12, 13). In addition, the halobacterial GvpC protein determines the shape of the gas vesicles (20). The roles of the other *gvp* genes and their products in gas vesicle synthesis have not yet been elucidated; however, there is strong evidence that *gvpD* and *gvpE* and their products are involved in the regulation of gas vesicle synthesis (10, 19, 23). (i) Transformation of the gas vesicle-negative *Haloferax volcanii* with various constructs containing p-*vac* genes revealed that p-*gvpDE* are not necessary for gas vesicle assembly; their absence, however, leads to a reduced amount of gas vesicles. A repressor function could be assigned to the 5′-terminal portion of the p-*gvpD* mRNA when it acts on p-*gvpFGHIJKLM* mRNA synthesis (19). (ii) Similarly, a deletion internal to mc-*gvpD* in the mc-*vac* region (ΔD) leads to an overproduction of gas vesicles in *Haloferax volcanii* transformants (10) and the addition of mc-*gvpD* again reduces the amount of gas vesicles to wild-type levels in such ΔD transformants (23), suggesting that GvpD is involved in the repression of gas vesicle synthesis.

* Corresponding author. Mailing address: Institut für Mikrobiologie und Genetik, Technische Hochschule Darmstadt, Schnittspahnstr. 10, D-64287 Darmstadt, Germany. Phone: (6151) 16-2957. Fax: (6151) 16-2956.

The p-*vac* region of *H. salinarium* PHH1 is transcribed as four units throughout growth: one transcript covers the p-*gvpFGHIJKLM* genes and occurs prior to the p-*gvpDE* mRNA, whereas the p-*gvpA* (and p-*gvpACNO*) transcripts are synthesized throughout the growth cycle (8, 19). The p-*gvpO* mRNA, starting at the promoter located at the 3′ end of p-*gvpN*, appears predominantly during exponential growth (20). Inspection of c-*gvpA* expression in *H. salinarium* PHH1 revealed that this promoter is inactive throughout the growth cycle (15). In *H. salinarium* PHH4, however, the c-*gvpA* mRNA is found during stationary growth and parallels the appearance of gas vesicles.

In this report, the expression of the entire c-*vac* region is investigated by analyzing the transcripts formed throughout the growth cycle of *H. salinarium* PHH4. In addition, the activity of the c-*gvpD* promoter is analyzed in wild-type *H. salinarium* PHH1. Antisera raised against the cGvpD and cGvpE proteins, synthesized in *Escherichia coli*, are used to assess the appearance of these proteins by Western blot (immunoblot) analysis. The two proteins are encoded by consecutive genes that are cotranscribed throughout the growth cycle, but surprisingly, they appear sequentially during the growth of *H. salinarium* PHH4. Antisense RNAs complementary to the c-*gvpD* region likewise appear at specific stages during growth and may inhibit the translation of c-*gvpD* mRNA.

## MATERIALS AND METHODS

**RNA isolation and Northern (RNA) analysis.** Isolation of total RNA from *H. salinarium* was carried out as described previously (8). For Northern analyses, the RNAs were separated on formaldehyde agarose gels (1). For probe generation, strand-specific RNAs were synthesized as recommended by Stratagene with recombinant Bluescript vectors containing a 236-bp *Kpn*I-*Dra*II fragment (AntiA), a 200-bp *Sac*II-*Bst*EII fragment (AntiDI), a 650-bp *Not*I-*Bst*EII fragment (DII), a 289-bp *Bam*HI fragment (AntiDIII), a *Sac*I-*Nru*I fragment (AntiD/E), and a 663-bp *Apa*I-*Pst*I fragment (AntiF). The following DNA fragments were labelled according to the random priming procedure with [α-$^{32}$P]dATP (11): the 236-bp *Kpn*I-*Dra*II fragment containing the c-*gvpA* gene (probe A), the 358-bp *Xho*I-*Sph*I fragment containing the c-*gvpN* gene (probe N), the 410-bp *Pvu*I-*Bam*HI fragment containing the c-*gvpO* gene (probe O), and the 860-bp *Xho*I fragment containing the c-*gvpIJK* genes (probe IJK).

**Preparation of protein crude extracts and Western blot analysis.** Total proteins of *H. salinarium* cells were isolated from 5-ml cell suspensions. The cell pellets were resuspended in 0.4 ml of Tris-EDTA buffer containing 10 μg of DNase I per ml and dialyzed overnight against distilled water. The dialyzed suspension was centrifuged for 20 min at 12,000 × *g* for membrane removal. Protein samples of 20 μg were separated on Tricine–sodium dodecyl sulfate (SDS)–16% polyacrylamide gels according to the method of Schägger and von Jagow (28). Western blot analyses were performed as described previously (10) by the enhanced chemiluminescence system from Amersham.

**Determination of the 5′ terminus of the c-*gvpD* mRNA by primer extension and S1 nuclease analysis.** The determination of the 5′ terminus of the c-*gvpD* mRNA by S1 nuclease analysis was done as described previously (8). For primer extension analysis, the cDNA was produced as described by Reiter et al. (24) with the Bethesda Research Laboratory reverse transcriptase kit, the 5′ $^{32}$P-labelled oligonucleotide 5′ TGGGGCACCGTTGACCA 3′ (positions 5816 to 5832 of the c-*vac* sequence; EMBL accession no. X94688), and total RNA. The labelled cDNA was analyzed on a 6% polyacrylamide sequencing gel along with a sequencing ladder generated with the above-described oligonucleotide as the primer.

**Determination of the 3′ terminus of the c-*gvpD* mRNA by S1 nuclease analysis.** For the generation of a labelled probe derived from the c-*gvpDE* region, a 544-bp fragment was amplified by PCR with two oligonucleotides (5′ GTATTCGGC GATGATGTCGTCGCCGAC 3′ and 5′ GCTACACGTCATTAGCATGG 3′). The fragment was cut with *Hin*fI and *Ava*I, yielding a 5′ overhang at the *Hin*fI site of a 261-bp c-*gvpD* fragment (positions 4517 to 4256 of the c-*vac* sequence). This probe could hybridize to the 3′ ends of transcripts starting from the c-*gvpD* promoter (8), ranging in size from 1,539 to 1,800 nucleotides (nt). After purification of the 261-bp fragment, the *Hin*fI site was labelled with [α-$^{32}$P]dATP with the Klenow enzyme; 500 ng of the *Hin*fI-*Ava*I DNA fragment was incubated in a solution containing 1× Fill-in buffer (U.S. Biochemicals), 0.1 mM dTTP, 30 μCi of [α-$^{32}$P]dATP, and 5 U of Klenow enzyme for 20 min at room temperature. The mixture was centrifuged through a P30 spin column. Hybridization and S1 nuclease digestion were carried out as described previously (15, 25). The sequence ladder was obtained with an oligonucleotide with the sequence 5′ GGGTCGGCAGCGAGAACTCCACGTCGGCGT 3′, which binds to nt 4374 to 4403 of the c-*vac* region (EMBL accession no. X94688).

**Expression of c-*gvpD* and c-*gvpE* in *E. coli*, isolation of the protein, and production of antibodies.** The c-*gvpD* gene was amplified by PCR with oligonucleotides containing *Bgl*II and *Hin*dIII sites (5′ GACCACACAGACAGATC TATGAGCGCACGC 3′ and 5′ GAGGTCGTCCAAGCTTTCACACCATCTC CGTGAG 3′; underlined sequences mark the respective restriction sites) and cloned into the pQE8 expression vector (Qiagen, Chatsworth, Calif.) which contains a 6-His-residue tag 5′ to the *Bam*HI cloning site. For the amplification of the c-*gvpE* gene, oligonucleotides containing *Bam*HI and *Hin*dIII sites were used (5′ CACGGAGATGGTGTGGATCCATGGACGACCTC 3′ and 5′ GCC GTACGTGTAGAGGTAAGCTTCACTCATCC 3′). The correct fusion of the translational reading frame with the His tag was confirmed in both cases by DNA sequencing. The *E. coli* strain M15(pREP4) (33) containing the repressor plasmid pREP4, which carries the *lacI* gene encoding the *lac* repressor, was transformed with the expression plasmid pQE8 × D or pQE8 × E, containing the c-*gvpD* or c-*gvpE* gene, respectively. An overnight culture of *E. coli* containing one of the above-described plasmids was diluted 1:10 in Luria broth containing 100 μg of ampicillin per ml and 25 μg of kanamycin per ml and grown at 37°C. Protein samples were drawn from the culture before and after induction with IPTG (isopropyl-β-D-thiogalactopyranoside) to a final concentration of 1 mM. After 4 h of growth, cells were collected by centrifugation, resuspended in phosphate-buffered saline, disrupted by pressure (in a French press; Aminco Co.), and again pelleted by centrifugation. The pellet was resuspended in a solution containing 7 M urea, 100 mM $NaH_2PO_4$, 5 mM β-mercaptoethanol, and 10 mM Tris-HCl (pH 8.0). The suspension was centrifuged, and the supernatant was loaded onto a nitrilotriacetic acid (NTA) column and washed with a wash buffer (7 M urea, 100 mM $NaH_2PO_4$, 5 mM β-mercaptoethanol, 10 mM Tris [pH 6.3]). In both cases the proteins were eluted from the column with wash buffer containing 250 mM imidazole and dialyzed against phosphate-buffered saline. Antibodies against the cGvpD protein were obtained by using chickens for immunization. Chickens were injected intramuscularly with up to 1 ml of solution containing 100 μg of recombinant protein in 0.5 ml mixed with 0.5 ml of complete Freund's adjuvant and given booster injections twice with 100 and 30 μg of protein, respectively. Polyclonal antibodies (immunoglobulin Y [IgY]) were purified from egg yolk in the following way: the intact yolk of one egg was washed with water to remove the egg white and then mixed thoroughly with 40 ml of Tris-buffered saline, incubated overnight at 4°C, and centrifuged (Heraeus centrifuge, 4,000 rpm, 20 min). Insoluble components were precipitated from the supernatant by addition of 3 ml of 10% dextran sulfate (in Tris-buffered saline) and 7.5 ml of 1 M $CaCl_2$ for 30 min at room temperature. The mixture was centrifuged as described above, and insoluble components were again precipitated by the addition of 3 ml of 10% dextran sulfate (in Tris-buffered saline). After another centrifugation step, the supernatant was used in a 1:1,000 dilution for Western blot analyses. For antiserum production against the cGvpE protein, a rabbit was injected with 100 μg of protein and given booster injections twice at intervals of 3 weeks. The antiserum was used in a 1:100 dilution for Western blot analyses.

## RESULTS

**Northern analyses to determine mRNAs derived from the c-*vac* region.** Total RNA of *H. salinarium* PHH4 was isolated from samples collected throughout the growth cycle (see Fig. 4) and investigated by Northern analyses. Samples were taken during exponential growth (samples 1 and 2), early stationary to mid-stationary growth (samples 3, 4, and 5), and late stationary growth (samples 6 and 7). Gas vesicles were first observed as light-refractile bodies in cells contained in sample 3, i.e., in the early stationary growth phase. The location of the probes used relative to the c-*vac* map is shown in Fig. 1A.

The Northern analyses were performed with RNAs from samples 2 to 7. The c-*gvpA*-specific probe indicated large amounts of the 0.34-kb c-*gvpA* transcript from early stationary to mid-stationary growth (samples 3 to 6), whereas during exponential growth no c-*gvpA* transcript was detectable (reference 15 and this report) (Fig. 1B, blot A). Almost no signal corresponding to c-*gvpA* mRNA was seen in the late stationary growth phase. In addition to the major 0.34-kb c-*gvpA* mRNA that has been described previously (15), larger transcripts were detected in smaller amounts: a more prominent 2.5-kb mRNA and fainter, smeary signals corresponding to transcripts of approximately 1.0 and 4.4 kb. The 2.5-kb transcript appeared in parallel with the c-*gvpA* mRNA. Since the same pattern of the larger transcripts was also seen with probes derived from the

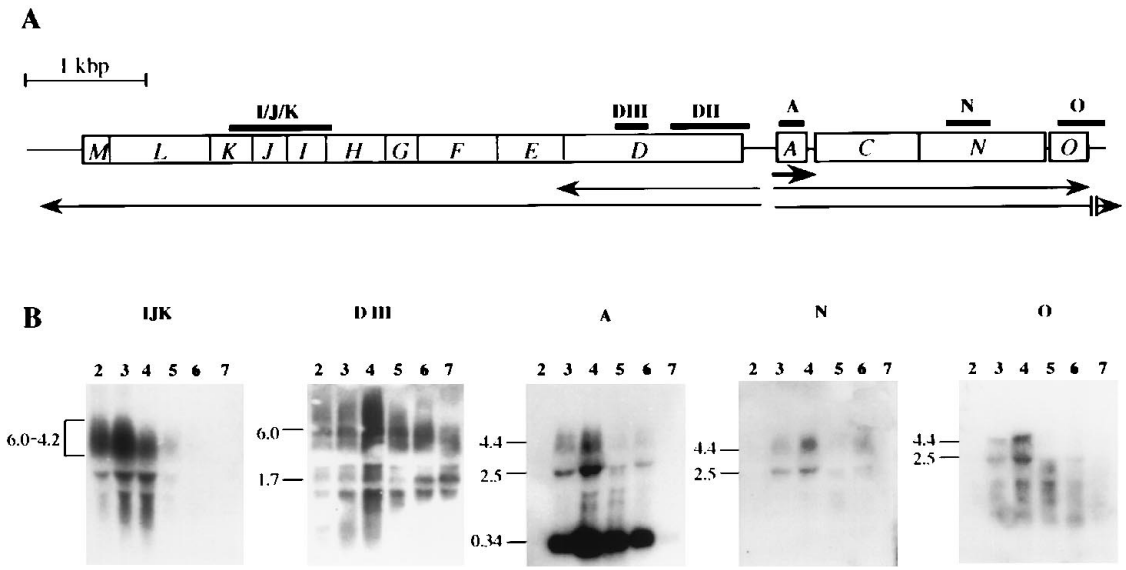


FIG. 1. Northern analyses of sense transcripts. (A) Schematic view of the c-*vac* region, with each *gvp* gene represented by a box. The names of the probes used for Northern hybridization are indicated over black bars above the respective genes and are described in Materials and Methods. The arrows underneath the map indicate the transcripts detected by Northern analyses. (B) For Northern analysis, 5 μg (blots A, N, and O) or 10 μg (blots DIII and IJK) of total RNA isolated during growth of *H. salinarium* PHH4 was separated on formaldehyde agarose gels. Numbers given above the Northern blots correspond to samples collected during various phases of growth (exponential [lane 2], stationary [lanes 3 and 4], and late stationary [lanes 6 and 7]). The blot labels (IJK, DIII, A, N, and O) reflect the names of the probes used. Numbers and lines on the left indicate the sizes (in kilobases) of the hybridizing mRNAs.

c-*gvpN* and c-*gvpO* genes (Fig. 1B, blots N and O), we assume that all transcripts initiate from the same site, determined to be 20 to 21 bp upstream of the ATG start codon of c-*gvpA* (15). The *gvpO* probe also detected smaller transcripts in minor amounts (Fig. 1B, blot O). The 0.34-kb transcript spans the c-*gvpA* gene, whereas the 2.5-kb transcript encompasses c-*gvpACNO*. The longer 4.4-kb RNA should also cover sequences located further downstream of c-*gvpO* (Fig. 1A).

Transcription of the c-*gvpDEFGHIJKLM* genes was investigated with various strand-specific RNA probes derived from c-*gvpD* and a DNA probe from the c-*gvpIJK* region. Aliquots of the same RNA samples used for the detection of the c-*gvpACNO* transcripts were investigated in these experiments. The c-*gvpD*-specific probe DIII (Fig. 1B, blot DIII) revealed hybridizing signals with sizes of up to 6 kb in all samples, indicating that the c-*gvpDEFGHIJKLM* genes were transcribed as relatively unstable mRNAs. An mRNA of 6 kb could span this entire gene cluster. Similar hybridization signals were also found in samples taken during early exponential growth (data not shown). The 23S and 16S rRNAs are visible as white spots in these Northern blots, and putative RNA species hybridizing around these areas are usually due to compressions. A transcript of 1.7 kb was, however, detected in the late stationary growth phase (Fig. 1B, blot DIII, lanes 6 and 7) and was also seen with probe DII derived from the 5′ end of the c-*gvpD* gene (data not shown). With the c-*gvpIJK*-specific probe, similar results were obtained: transcripts of up to 6 kb were detected in samples 2 to 4, but the size decreased in sample 5, whereas samples 6 and 7 did not indicate hybridization signals (Fig. 1B, blot IJK). These results suggested that RNA degradation (also observed in samples 6 and 7 with the DIII probe) occurred predominantly from the 3′ ends of the mRNAs. The 1.7-kb c-*gvpD* mRNA species seen in samples 6 and 7 with the DIII probe cannot be visualized with the IJK probe.

**Determination of the 5′ and 3′ termini of the 1.7-kb c-*gvpD* mRNA.** The start site of the c-*gvpDEFGHIJKLM* mRNA has been mapped previously and lies 116 nt upstream of the ATG start codon of the c-*gvpD* gene (8). To determine whether the 1.7-kb transcript observed with the DIII probe (and also with probe DII [data not shown]) (Fig. 1) starts at the same promoter, S1 nuclease mapping and primer extensions were performed (Fig. 2A). Protected fragments and cDNA signals were observed with all investigated RNA samples, implying that the c-*gvpD* promoter is active from exponential up to stationary growth. The length of the cDNA was in both cases 231 nt, locating the start site at the same site, 116 nt upstream of c-*gvpD*.

S1 nuclease protection studies were also done to determine the 3′ terminus of the 1.7-kb c-*gvpD* mRNA (Fig. 2B). RNAs isolated from samples 2 to 7 were analyzed with a 3′ end-labelled 261-bp *Hin*fI-*Ava*I fragment from the c-*gvpDE* region. The highest amount of the protected hybrid was found with sample 7, which also corresponds to the data obtained by Northern analyses (Fig. 1B, blot DIII). The size of this RNA-DNA hybrid was 178 bp, locating the 3′ terminus of the c-*gvpD* transcript 1,716 nt downstream of the transcriptional start site of c-*gvpD* and 120 nt downstream of the TGA stop codon of the c-*gvpD* gene, at the second adenosine of the sequence 5′ ATCGACGAC 3′ (Fig. 2C). A stem-loop structure which might be involved in the termination of the 1.7-kb c-*gvpD* mRNA could form 7 nt upstream of this termination site.

**Expression of c-*gvpD* and c-*gvpE* in *E. coli*, and isolation of both proteins for antibody formation.** To investigate the expression of the c-*gvpDE* genes at the protein level, antibodies were raised against cGvpD and cGvpE, synthesized in *E. coli* with the pQE8 expression vector system (Qiagen). The recombinant proteins contained N-terminal 6-His-residue tags, and purification was performed under denaturing conditions (Fig. 3). Protein samples were drawn from the culture before and after induction with IPTG (Fig. 3A, lanes 1 and 2 for cGvpD). Cells were disrupted by pressure, and the proteins were solubilized with urea (Fig. 3A, lane 5 for cGvpD; Fig. 3B, lane 2 for cGvpE). This suspension was loaded onto an NTA column, and the proteins were eluted with wash buffer containing im-

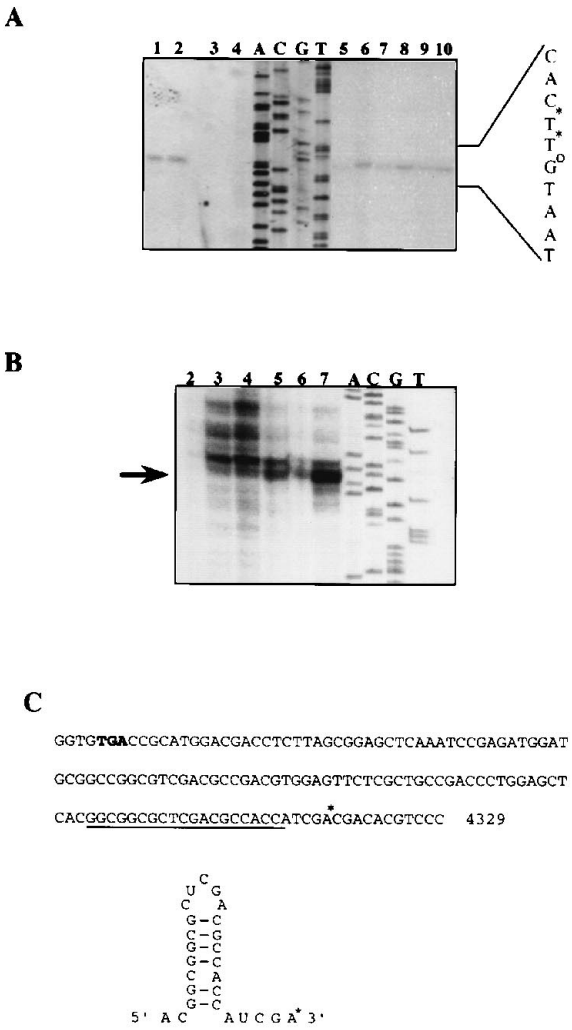


FIG. 2. S1 nuclease and primer extension analysis to determine the 5′ end (A) and 3′ end (B) of the 1.7-kb c-*gvpD* mRNA and the nucleotide sequence of the region downstream of the c-*gvpD* stop codon around the termination site (C). The oligonucleotides used for the generation of the probe are described in Materials and Methods. (A) S1 nuclease mapping (lanes 1 to 4) and primer extension analysis (lanes 5 to 10) to determine the 5′ terminus. The RNA used for S1 nuclease analysis derived from the early exponential phase of *H. salinarium* PHH4. Lane 1, 0.5 μg of RNA; lane 2, 1 μg of RNA; lane 3, 0 μg of RNA; lane 4, 15,000 cpm-labelled DNA. The RNAs used for primer extension analysis derived from *H. salinarium* PHH4 sample 3 (lanes 5 and 6), sample 4 (lanes 7 and 8), and sample 6 (lanes 9 and 10). Lanes 5, 7, and 9, 10 μg of RNA; lanes 6, 8, and 10, 20 μg of RNA. The sequencing ladder in lanes marked A, C, G, and T was generated with the same primer as that used for the primer extension analysis. The asterisk in the complementary DNA sequence marks the 5′ terminus as determined by S1 nuclease analysis; the circle indicates the end of the cDNA as determined by primer extension analysis. (B) Determination of the 3′ end. In lanes 2 to 7, 10 μg of RNA of *H. salinarium* PHH4 derived from samples 2 to 7 was hybridized with 50,000 cpm of the c-*gvpD* probe and digested with S1 nuclease. The sequence ladder (in lanes marked A, C, G, and T) was obtained as described above. The arrow indicates the protected fragment of 178 nt. (C) 3′-terminal DNA sequence of the c-*gvpD* gene with the TGA stop codon (in boldface type) and adjacent sequences. The numbering on the right side is according to the c-*vac* sequence. The asterisk indicates the termination site of the c-*gvpD* mRNA. The possible stem-loop structure formed by the underlined sequence upstream of the termination site is shown underneath.

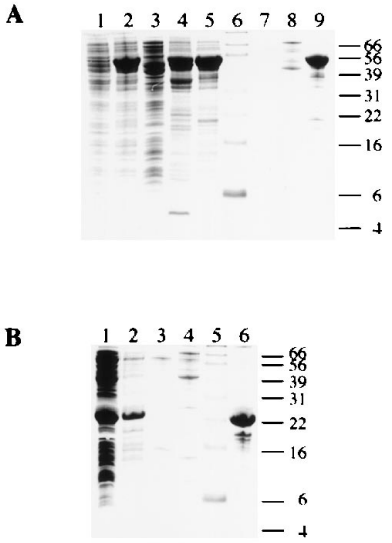


FIG. 3. Purification procedure of cGvpD and cGvpE from *E. coli*. (A) SDS-polyacrylamide gel electrophoresis (PAGE) of crude extracts of *E. coli* pQE8 × D and purification procedure of the c-GvpD protein. Lane 1, cell lysates of *E. coli* pQE8 × D before induction with IPTG; lane 2, 4 h after induction with IPTG; lane 3, soluble crude extract of *E. coli* pQE8 × D protein after disruption by pressure; lane 4, insoluble crude extract of *E. coli* pQE8 × D protein after disruption by pressure; lane 5, solubilized crude extract after treatment with 7 M urea; lane 6, protein markers (sizes in kilodaltons are indicated at the right side); lane 7, flow-through of protein extract after loading onto the NTA column; lane 8, flow-through of proteins after washing with wash buffer; lane 9, purified fusion protein after elution from the NTA column with imidazole. (B) SDS-PAGE of cell lysates of *E. coli* pQE8 × E and purification of the c-GvpE protein. Lane 1, soluble crude extract of *E. coli* pQE8 × E protein after disruption by pressure; lane 2, soluble crude extract of *E. coli* pQE8 × E protein after treatment with 7 M urea; lane 3, flow-through of proteins after loading onto the NTA column; lane 4, flow-through of proteins from the NTA column after washing with wash buffer; lane 5, protein markers (sizes in kilodaltons are indicated at the right side); lane 6, purified fusion protein after elution from the NTA column with imidazole.

idazole (Fig. 3A, lane 9 for cGvpD; Fig. 3B, lane 6 for cGvpE). Because of the 6-His-residue tag, both fusion proteins were 930 Da larger than the proteins deduced from the c-*gvpD* sequence (54 kDa) or the c-*gvpE* sequence (21 kDa). The anti-cGvpD antibodies were formed in chickens, whereas the anti-cGvpE antiserum was produced in rabbits.

**Detection of c-GvpD, c-GvpE, and c-GvpA in *H. salinarium* PHH4.** *H. salinarium* PHH4 crude extracts used for Western blot analyses were prepared from the same samples taken throughout the growth cycle for the Northern analyses (Fig. 4). For comparison, the appearances of cGvpA and gas vesicles were monitored throughout the growth cycle by Western blot analysis with an antiserum raised against isolated gas vesicles from *Haloferax mediterranei* (10).

**Detection of cGvpD.** Prior to the immunization of the chickens with the purified cGvpD protein, the IgY fraction was tested for nonspecific binding with protein sample 1 of *H. salinarium* PHH4 and the purified cGvpD protein of *E. coli* (Fig. 4, blot GvpD, control lanes D and 1). No reaction was seen with the purified cGvpD protein from *E. coli*, whereas in *H. salinarium* sample 1, the pre-IgY fraction detected two protein bands because of a nonspecific binding (Fig. 4, blot GvpD, control lane 1). With the anti-cGvpD IgY fraction for a similar Western blot analysis, a strong reaction was found with the cGvpD protein purified from *E. coli* (Fig. 4, blot GvpD, noncontrol lane D). Binding signals were observed with a protein of the expected size (54 kDa) in protein samples of *H. salinarium* PHH4 obtained from the early exponential growth phase (Fig. 4, blot GvpD, noncontrol lanes 0 and 1); the signal declined in samples 2 and 3 and remained low up to late stationary growth (Fig. 4, blot GvpD). A protein sample taken

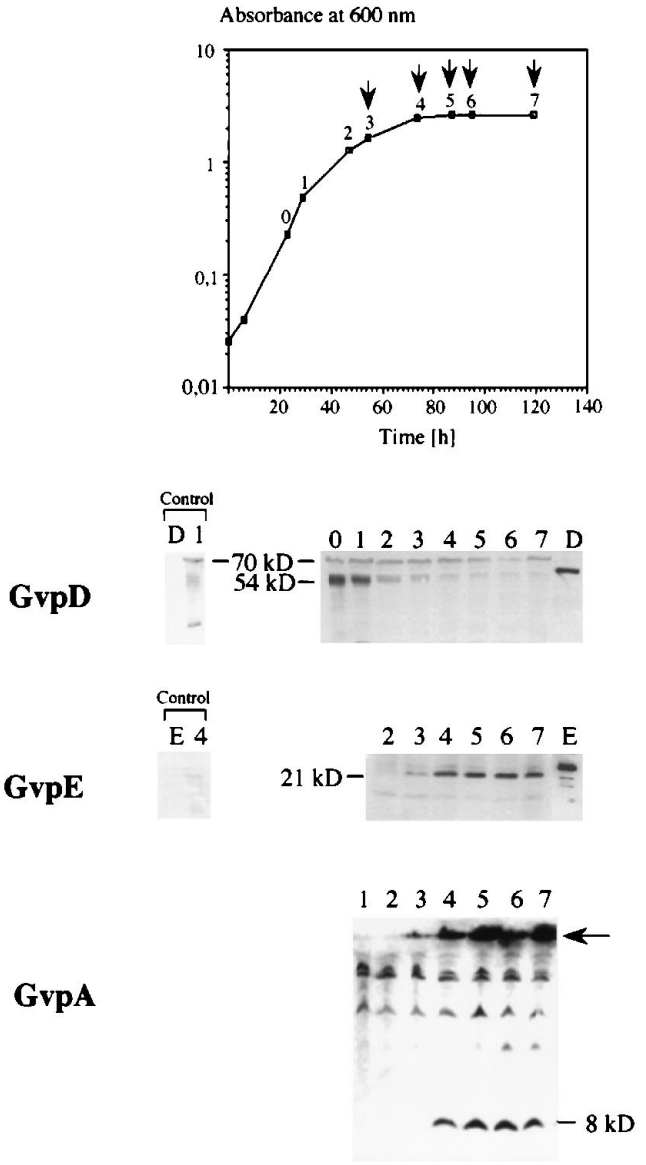


FIG. 4. Growth-dependent sampling of *H. salinarium* PHH4 cells, and Western blot analysis of cell lysates using anti-cGvpD (GvpD), anti-cGvpE (GvpE), and anti-gas vesicle (GvpA) antisera. Growth curve for the culture development of *H. salinarium* PHH4 depicting the sampling course for microscopic observation and protein and RNA isolation. Numbers 0 to 7 indicate the time points when samples were taken, and arrows designate the points in the growth cycle when cGvpA was detectable by Western blot analysis and gas vesicles were visible. Numbers above lanes 0 to 7 in each Western blot correspond to these protein samples. Twenty micrograms of protein was applied in each slot. In blot GvpD, lanes designated D contain the purified cGvpD protein isolated from *E. coli* pQE8 × D. Proteins in the control lanes were probed with antibodies obtained from egg yolk prior to the immunization, whereas the noncontrol lanes were treated with the anti-cGvpC antiserum. In blot GvpE, lanes designated E contain the purified cGvpE protein isolated from *E. coli* pQE8 × E. Proteins in the control lanes were probed with antiserum obtained from a rabbit prior to immunization, whereas the noncontrol lanes were treated with the anti-cGvpE antiserum. In blot GvpA, the expression of cGvpA was assessed with the anti-gas vesicle antiserum described by Englert et al. (10). The arrow indicates the reaction of the antiserum with GvpA aggregates and partially disaggregated gas vesicles. The 8-kDa marker designates the cGvpA monomer.

in the very late stationary growth phase (after 240 h) showed no cGvpD protein (data not shown). Thus, cGvpD is primarily synthesized during exponential growth, when c-*gvpA* mRNA and gas vesicles are not present. The 1.7-kb c-*gvpD* mRNA that appeared in late stationary growth was obviously not translated into cGvpD protein.

**Detection of cGvpE.** The preimmune serum taken before immunization was tested with sample 4 of *H. salinarium* PHH4 and with the purified cGvpE protein of *E. coli* (Fig. 4, blot GvpE; control lanes E and 4). No reaction was seen with either sample. Western blot analysis using the anti-cGvpE antiserum indicated a strong hybridization signal with the purified cGvpE protein from *E. coli* (Fig. 4, blot GvpE, noncontrol lane E). As expected, this protein was slightly larger (due to the 6-His-residue tag) than the size of cGvpE deduced from the c-*gvpE* sequence. Protein samples of *H. salinarium* PHH4 showed no hybridization in sample 2, a weak hybridization signal in sample 3, and a strong signal corresponding to the expected size of 21 kDa in samples 4 to 7 (Fig. 4, blot GvpE). The sample taken in the very late stationary growth phase (after 240 h) again indicated no cGvpE protein (data not shown). Thus, cGvpE was present in *H. salinarium* PHH4 during stationary growth and occurred parallel to the synthesis of cGvpA (see below).

**Detection of cGvpA.** For comparison, the anti-gas vesicle antiserum raised against isolated gas vesicles from *Haloferax mediterranei* was applied. This antiserum detects the major 8-kDa gas vesicle structural protein, GvpA, in all gas vesicle-producing halobacteria (10). The cGvpA protein was detected in samples 4 to 7, and aggregates of GvpA and partially disaggregated gas vesicles were detectable already in sample 3 (Fig. 4, blot GvpA). Such GvpA aggregates can also be observed with protein samples of *Haloferax mediterranei*, *H. salinarium* PHH1, or cyanobacterial gas vesicles (10, 19, 32). Nonspecific reactions were seen with all samples.

In summary, these results indicated that, despite the fact that the c-*gvpDEFGHIJKLM* mRNA was present throughout growth, the first two proteins encoded by this mRNA appeared at different times during the growth cycle: the cGvpD protein was present only during early exponential growth whereas the cGvpE protein occurred during stationary growth parallel to cGvpA and gas vesicle formation.

**Presence of GvpD and GvpE in wild-type *H. salinarium* PHH1.** The presence of cGvpD and cGvpE in *H. salinarium* PHH1 was assessed with the same antisera described above. Soluble proteins were isolated from samples collected throughout the growth of *H. salinarium* PHH1 and used for Western blot analysis. With the anti-cGvpD antibodies, a strong reaction was found with a protein of a size similar to that determined for cGvpD (54 kDa), which appeared in the exponential growth phase (Fig. 5, lanes 1 to 3), and less strong reactions were observed up to the mid-stationary growth phase (Fig. 5, lanes 4 to 6). No reaction was seen in samples taken from the late stationary growth phase (Fig. 5, lanes 6 and 7). As observed with *H. salinarium* PHH4, the binding with the 70-kDa protein was again caused by nonspecific cross-reactions. Since a protein sample of a *Haloferax volcanii* transformant expressing the p-*vac* region showed no binding with the anti-cGvpD antibodies (data not shown) and the p-*gvpDE* genes are transcribed in stationary growth only (19), these results indicate that the cGvpD protein must be synthesized in *H. salinarium* PHH1. With the anti-cGvpE antiserum in a similar Western blot analysis, no reactions could be detected (Fig. 5, blot GvpE). Thus, the cGvpE protein is not present in *H. salinarium* PHH1.

**Detection of antisense RNAs in the c-*gvpADEF* region in *H. salinarium* PHH4.** For the detection of putative antisense RNAs complementary to the c-*gvpDE* region of the c-*gvpDEFGHIJKLM* mRNA, strand-specific RNA probes were used for Northern analyses. The positions of the probes and the results of these experiments are presented in Fig. 6. With the probes

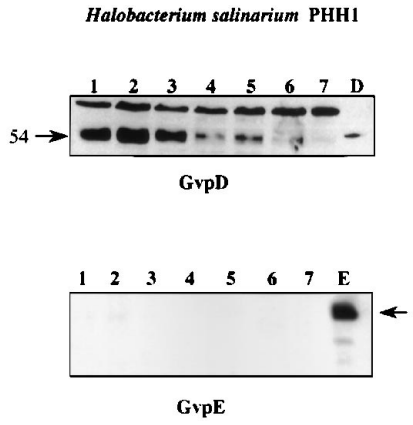


FIG. 5. Western blot analysis of wild-type *H. salinarium* PHH1 cell lysates using anti-cGvpD and anti-cGvpE antisera. Twenty micrograms of protein was applied in each slot. Total proteins were isolated throughout the growth cycle. Lanes show growth phases as follows: early exponential (lane 1), exponential (lanes 2 and 3), late exponential (lane 4), early stationary (lane 5), stationary (lane 6), and late stationary (lane 7). The lanes designated D and E contain the purified cGvpD or cGvpE protein isolated from *E. coli* pQE8 × D or *E. coli* pQE8 × E, respectively. The arrow at the left of blot GvpD indicates the 54-kDa cGvpD protein; the arrow at the right of blot GvpE marks the cGvpE protein.

AntiF and AntiA for Northern analyses, no hybridization signals could be detected (data not shown). Antisense RNAs were, however, observed with probes specific for the 5′-terminal portion of the c-*gvpD* mRNA (AntiDI) and for the 3′ portion of the c-*gvpD* mRNA (AntiD/E) (Fig. 6). The AntiDI probe indicated two small RNAs of 0.28 and 0.19 kb in samples 2 to 4, i.e., at the transition from late exponential to stationary growth, parallel to gas vesicle synthesis and the decline of the cGvpD protein. Neither sample 1 nor samples 5 to 7 contained these two RNAs, but both appeared in large amounts in samples 3 and 4 (Fig. 6, blot AntiDI). Also, the AntiD/E probe indicated RNAs of 0.28 and 0.18 kb most strongly in samples 3 and 4 but not in sample 2 or in samples 6 and 7 (Fig. 6, blot

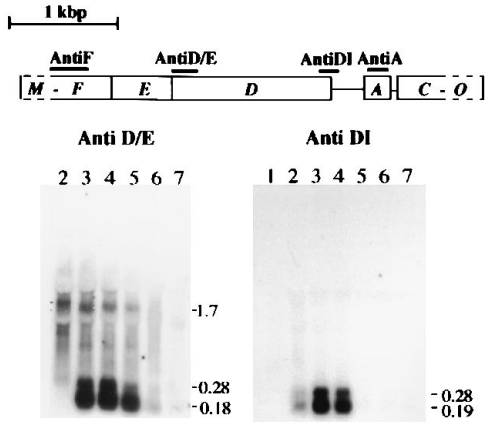


FIG. 6. Northern analyses for the detection of antisense RNAs in the c-*gvpADEF* region. The names of the probes used for these hybridizations are indicated over black bars above the respective genes. For Northern analyses (lower part), total RNAs (10 μg each) isolated during the growth cycle (Fig. 4) were separated on formaldehyde agarose gels. Numbers above the Northern blots correspond to the samples taken during growth. Only Northern blots that gave signals are presented; the AntiF and AntiA probes did not reveal any hybridization signal (data not shown). Lines and numbers at the right of the Northern blots indicate the sizes (in kilobases) of the hybridizing antisense RNAs.

AntiD/E). The search for DNA sequence similarities between the c-*gvpD* 5′ region and the region hybridizing with the antiD/E probe revealed no similarities. Thus, the two antisense RNAs detected with both probes were clearly different.

## DISCUSSION

Gas vesicle synthesis in halobacteria is a process of unexpected complexity: it requires the activity of 14 *gvp* genes organized as two clusters. One cluster comprises the genes c-*gvpACNO*, and the second unit, oriented in the opposite direction, comprises the genes c-*gvpDEFGHIJKLM* (4, 8). In this study we investigated the transcription of the entire c-*vac* region in *H. salinarium* PHH4 and analyzed the expression of the two genes c-*gvpD* and c-*gvpE* at the protein level. Recent studies showed that both Gvp proteins are involved in the regulation of gas vesicle synthesis (10, 17, 19, 23, 26).

The c-*gvpACNO* gene cluster is transcribed from a start site located 20 to 21 bp upstream of the c-*gvpA* start codon (15), resulting in the major 0.34-kb c-*gvpA* transcript and a minor transcript of 2.5 kb spanning c-*gvpACNO*. Longer transcripts also cover additional sequences further downstream. These transcripts are possibly due to read-through of a putative termination signal, as is often found for archaeal transcript termination (6, 24). The transcription pattern of c-*gvpACNO* differs slightly from the expression of the mc-*gvpACNO* genes in *Haloferax mediterranei*. Besides the major transcript encompassing the mc-*gvpA* gene, three additional mRNA species appear covering mc-*gvpAC*, mc-*gvpACN*, and mc-*gvpACNO*; all formed because of read-through of termination signals (9, 26). The plasmid-borne p-*gvpACNO* operon of *H. salinarium* PHH1 contains in addition to the p-*gvpA* promoter (leading to the major p-*gvpA* and the minor p-*gvpACNO* transcripts) a further promoter in front of p-*gvpO*, underlining the importance of this gene for gas vesicle synthesis (20). The deletion of DNA sequences located further downstream of p-*gvpO* or mc-*gvpO* has no effect on gas vesicle formation, whereas the deletion of *gvpO* always results in Vac-negative transformants, indicating that the *gvpO* gene represents the boundary of the *vac* region (10, 20). In the gas vesicle-synthesizing cyanobacterium *Calothrix* species PCC 7601, the *gvpA* and *gvpC* genes in the *gvpA1A2C* operon are cotranscribed and an antisense RNA covering *gvpA1* and *gvpA2* might be involved in the regulation of their expression (2, 3). No antisense RNA covering *gvpA* is, however, detectable for these genes in halobacteria (references 20 and 26 and this report).

The second transcriptional unit of the c-*vac* region comprises the genes c-*gvpDEFGHIJKLM*, which were transcribed as one unit throughout growth, resulting in a relatively unstable mRNA. No additional promoter could be detected in the c-*gvpEF* region, as was found for the p-*vac* region (19). The c-*gvpD* promoter is active throughout growth; thus, the c-*gvp DEFGHIJKLM* mRNA is already present during exponential growth and prior to the formation of c-*gvpA* and c-*gvpACNO* mRNAs. In late stationary growth, an additional transcript of 1.7 kb covering c-*gvpD* was formed. The transcription of the *gvpD* to *gvpM* genes is similar in *Haloferax mediterranei*, in which one promoter active throughout growth drives expression (8, 26). Again, transcription in the p-*vac* region of *H. salinarium* PHH1 is different, since the p-*gvpDEFGHIJKLM* genes are differentially transcribed as two units. In this regard, the p-*gvpFGHIJKLM* mRNA occurs exclusively during exponential growth whereas the p-*gvpDE* mRNA is found only in stationary growth (19).

Monitoring the cGvpD protein level in *H. salinarium* PHH4 revealed an unexpected result: despite the presence of an

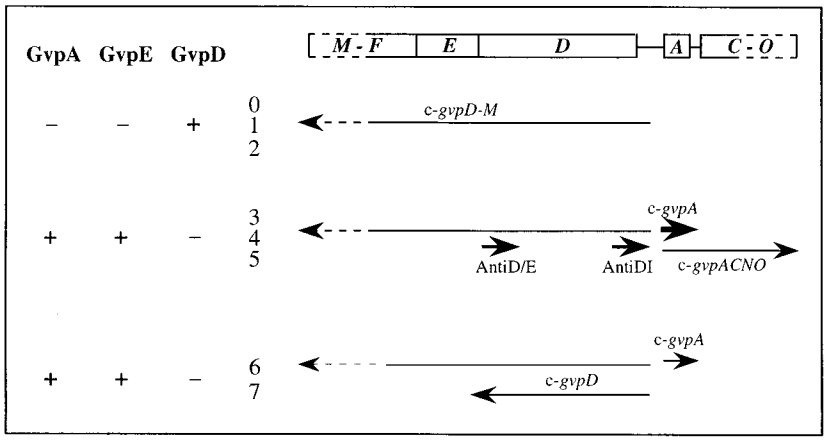


FIG. 7. Scheme of the protein content and diagram of c-*vac* transcripts during growth of *H. salinarium* PHH4. + and − refer to the presence or absence of cGvpA, cGvpE, and cGvpD. The numbers stand for samples taken during the growth cycle that are from early to late exponential growth phases (0, 1, and 2), early to stationary growth phases (3, 4, and 5), and late stationary growth phase (6 and 7). The transcripts are depicted as arrows, whose thicknesses differentiate between large or small amounts of transcripts. The arrows designated AntiD/E and AntiDI indicate the approximate positions of the hybridizing antisense RNAs.

mRNA covering c-*gvpD* throughout growth (as part of the 6-kb c-*gvpDEFGHIJKLM* or 1.7-kb c-*gvpD* mRNA), the cGvpD protein is detectable only during early exponential growth, up to approximately 24 h before the c-*gvpA* mRNA appears and gas vesicles are formed. Since the amount of cGvpD is much smaller from that time point on up to the late stationary phase, the translation of the mRNA into cGvpD must somehow be inhibited. Moreover, we observed a growth-phase-dependent characteristic of cGvpE, because the cGvpE protein was not present during exponential growth but occurred in stationary growth parallel to the formation of cGvpA. Thus, the two genes located near the 5′ end of the c-*gvpDEFGHIJKLM* mRNA were translated at different times during growth. The mechanisms leading to this differential synthesis are still under investigation, but in the case of c-*gvpD*, antisense RNAs might interfere with the translation into protein.

Such antisense RNAs complementary to the 5′- and 3′-terminal parts of c-*gvpD* appeared during early stationary phase parallel to the decline of the amount of cGvpD protein. It is possible that translation of the c-*gvpD* mRNA is inhibited because of binding of these antisense RNAs to the mRNA, whereas the expression of the remaining reading frames of the c-*gvpDEFGHIJKLM* transcript (as shown for c-*gvpE*) remains unimpaired. The antisense RNAs could mediate their function by the formation of RNA-RNA hybrids to prevent efficient translation, but these RNA-RNA hybrids could also be targets for subsequent cleavage by a specific RNase. Such a double-stranded/single-stranded-specific RNase activity has already been identified in *H. salinarium*. This enzyme acts, e.g., during lysogenic growth of the halobacterial phage ϕH in which, because of the presence of an appropriate antisense RNA, the 5′-terminal part of the early lytic mRNA is removed by a specific cleavage (29, 30).

However, the 1.7-kb c-*gvpD* mRNA that appeared in stationary growth was not translated into protein, although no antisense RNAs could be detected during these stages of growth. In addition, a similar correlation with the appearance of antisense RNAs and inhibition of c-*gvpE* mRNA translation was not possible since no antisense RNAs were detected during early stages of growth (17). Thus, the reason for the lack of c-*gvpE* translation during exponential growth still needs to be elucidated, but it is also possible that the cGvpD protein is involved in this process.

The appearance of the two proteins cGvpD and cGvpE was also investigated with wild-type *H. salinarium* PHH1. In contrast to the c-*gvpA* promoter, which remains inactive in this strain, the c-*gvpD* promoter was active (as determined by S1 nuclease analysis [data not shown]) and cGvpD protein was subsequently detectable during growth. No cGvpE protein was, however, present, which is most probably the reason why the c-*gvpA* promoter remains inactive in this strain, since the cGvpE protein is required as the transcriptional activator for the activity of the c-*gvpA* promoter. This has been directly demonstrated by transformation experiments and was also observed with the mc-*vac* region (17, 26). Thus, *H. salinarium* PHH1 does not contain c-*vac*-encoded gas vesicles.

Combining the results presented here with previous data, the expression of the c-*vac* region in *H. salinarium* PHH4 takes the following pattern (Fig. 7). During exponential growth phase (Fig. 7, samples 0, 1, and 2), the c-*gvpA* promoter is inactive and no gas vesicles appear (15). The lack of c-*gvp ACNO* transcription in this stage of growth is due to the absence of the cGvpE activator protein, required for c-*gvpA* promoter activation (17). The c-*gvpDEFGHIJKLM* genes are transcribed, but the translation of c-*gvpE* is inhibited. In contrast, the cGvpD protein, which is involved in the repression of gas vesicle synthesis, is present during exponential growth. In the stationary growth phase (Fig. 7, samples 3, 4, and 5), the amount of cGvpD is strongly reduced. At the same time, various antisense RNAs complementary to the c-*gvpD* mRNA appear and might prevent its efficient translation into cGvpD. Parallel to the decline of the cGvpD protein, the cGvpE protein is synthesized at this time, leading to the transcriptional activation of the c-*gvpA* promoter and the subsequent formation of c-*gvpA* as well as c-*gvpACNO* mRNA, followed by gas vesicle synthesis. During late stationary growth (Fig. 7, samples 6 and 7) the amounts of the different antisense RNAs are strongly reduced. A 1.7-kb c-*gvpD* mRNA occurs, which is, however, not translated into cGvpD protein.

The regulation of c-*vac*-encoded gas vesicle synthesis is complex and involves different factors acting either at the transcriptional level (such as cGvpE [17, 26]) or at the translational level (possibly mediated by antisense RNAs), as implied by the observations described here. Further experiments are, however, necessary to uncover the reason(s) for the differential

synthesis of the two regulatory gas vesicle proteins cGvpE and cGvpD.

## ACKNOWLEDGMENTS

Part of this work was performed at the Max-Planck-Institut für Biochemie in Martinsried, Germany, and we thank Wolfram Zillig for hospitality and discussions. Martin Lanzendörfer, Sonja Offner, and Richard Röder are thanked for helpful suggestions, and Kathryn Nixdorff is thanked for a critical reading of the manuscript.

This work was financially supported by the Deutsche Forschungsgemeinschaft (SFB 145/B6 and Pf 165/6-1).

## REFERENCES

1. **Ausubel, F., R. Brent, R. Kingston, D. Moore, J. Seidman, J. A. Smith, and K. Struhl (ed.).** 1989. Current protocols in molecular biology. Greene Publishing Associates and Wiley-Interscience, New York.
2. **Csizar, K., J. Houmard, T. Damerval, and N. Tandeau de Marsac.** 1987. Transcriptional analysis of the cyanobacterial *gvpABC* operon in differentiated cells: occurrence of an antisense RNA complementary to three overlapping transcripts. Gene **60:**29–37.
3. **Damerval, T., G. Gugliemi, J. Houmard, and N. Tandeau de Marsac.** 1991. Hormogonium differentiation in the cyanobacterium *Calothrix*: a photoregulated developmental process. Plant Cell **3:**191–201.
4. **DasSarma, S., P. Arora, F. Lin, E. Molinari, and L. R.-S. Yin.** 1994. Wild-type gas vesicle formation requires at least ten genes in the *gvp* gene cluster of *Halobacterium halobium* plasmid pNRC100. J. Bacteriol. **176:**7646–7652.
5. **DasSarma, S., T. Damerval, J. G. Jones, and N. Tandeau de Marsac.** 1987. A plasmid-encoded gas vesicle protein gene in a halophilic archaebacterium. Mol. Microbiol. **1:**365–370.
6. **DasSarma, S., U. RajBhandary, and H. G. Khorana.** 1984. Bacterio-opsin mRNA in wild-type and bacterio-opsin-deficient *Halobacterium halobium* strains. Proc. Natl. Acad. Sci. USA **81:**125–129.
7. **Englert, C., M. Horne, and F. Pfeifer.** 1990. Expression of the major gas vesicle protein gene in the halophilic archaebacterium *Haloferax mediterranei* is modulated by salt. Mol. Gen. Genet. **222:**225–232.
8. **Englert, C., K. Krüger, S. Offner, and F. Pfeifer.** 1992. Three different but related gene clusters encoding gas vesicles in halophilic archaea. J. Mol. Biol. **227:**586–592.
9. **Englert, C., and F. Pfeifer.** 1993. Analysis of gas vesicle gene expression in *Haloferax mediterranei* reveals that GvpA and GvpC are both gas vesicle structural proteins. J. Biol. Chem. **268:**9329–9336.
10. **Englert, C., G. Wanner, and F. Pfeifer.** 1992. Functional analysis of the gas vesicle gene cluster of the halophilic archaeon *Haloferax mediterranei* defines the vac-region boundary and suggests a regulatory role for the *gvpD* gene or its product. Mol. Microbiol. **6:**3543–3550.
11. **Feinberg, A. P., and B. Vogelstein.** 1983. A technique for radiolabelling DNA restriction fragments to high specific activity. Anal. Biochem. **132:**6–13.
12. **Halladay, J., J. Jones, F. Lin, B. MacDonald, and S. DasSarma.** 1993. The rightward gas vesicle operon in *Halobacterium* plasmid pNRC100: identification of the *gvpA* and *gvpC* gene products by use of antibody probes and gentic analysis of the region downstream of *gvpC*. J. Bacteriol. **175:**684–692.
13. **Hayes, P. K., B. Buchholz, and A. E. Walsby.** 1992. Gas vesicles are strengthened by the outer surface protein GvpC. Arch. Microbiol. **157:**229–234.
14. **Horne, M., C. Englert, C. Wimmer, and F. Pfeifer.** 1991. A DNA region of 9 kbp contains all genes necessary for gas-vesicle synthesis in halophilic archaebacteria. Mol. Microbiol. **5:**1159–1174.
15. **Horne, M., and F. Pfeifer.** 1989. Expression of two gas vacuole protein genes in *Halobacterium halobium* and other related species. Mol. Gen. Genet. **218:**437–444.
16. **Jones, J., D. Young, and S. DasSarma.** 1991. Structure and organization of the gas vesicle gene cluster on the *Halobacterium halobium* plasmid pNRC100. Gene **102:**117–122.
17. **Krüger, K., and F. Pfeifer.** Unpublished results.
18. **Mwatha, W. E., and W. D. Grant.** 1993. *Natronobacterium vacuolata* sp. nov., a haloalkaliphilic archaeon isolated from Lake Magadi, Kenya. Int. J. Syst. Bacteriol. **43:**401–404.
19. **Offner, S., and F. Pfeifer.** 1995. Complementation studies with the gas vesicle encoding p-vac region of *Halobacterium salinarium* PHH1 reveal a regulatory role for the p-*gvpDE* genes. Mol. Microbiol. **16:**9–19.
20. **Offner, S., G. Wanner, and F. Pfeifer.** 1996. Functional studies of the p-*gvpACNO* operon of *Halobacterium salinarium* reveal that the GvpC protein shapes gas vesicles. J. Bacteriol. **178:**2071–2078.
21. **Pfeifer, F., and U. Blaseio.** 1989. Insertion elements and deletion formation in a halophilic archaebacterium. J. Bacteriol. **171:**5135–5140.
22. **Pfeifer, F., and P. Ghahraman.** 1993. Plasmid pHH1 of *Halobacterium salinarium*: characterization of the replicon region, the gas vesicle gene cluster and insertion elements. Mol. Gen. Genet. **238:**193–200.
23. **Pfeifer, F., S. Offner, K. Krüger, P. Ghahraman, and C. Englert.** 1994. Transformation of halophilic archaea and investigation of gas vesicle synthesis. Syst. Appl. Microbiol. **16:**569–577.
24. **Reiter, W.-D., P. Palm, and W. Zillig.** 1988. Transcription termination in the archaebacterium *Sulfolobus*: signal structures and linkage to transcription initiation. Nucleic Acids Res. **16:**2454–2459.
25. **Reiter, W.-D., P. Palm, W. Voos, J. Kaniecki, B. Grampp, W. Schulz, and W. Zillig.** 1987. Putative promoter elements for the ribosomal RNA genes of the thermoacidophilic archaebacterium *Sulfolobus* sp. strain B12. Nucleic Acids Res. **14:**5581–5595.
26. **Röder, R., and F. Pfeifer.** Influence of salt on the transcription of the gas vesicle genes of *Haloferax mediterranei* and identification of the endogenous transcriptional activator gene. Microbiology, in press.
27. **Rodriguez-Valera, F., G. Juez, and D. Kushner.** 1983. *Halobacterium mediterranei* sp. nov., a new carbohydrate-utilizing extreme halophile. Syst. Appl. Microbiol. **4:**369–381.
28. **Schägger, H., and G. von Jagow.** 1987. Tricine-sodium dodecyl sulfate-polyacrylamide gel electrophoresis for the separation of proteins in the range from 1 to 100 kDa. Anal. Biochem. **166:**368–379.
29. **Stolt, P., and W. Zillig.** 1993. Antisense RNA mediates transcriptional processing in an archaebacterium, indicating a novel kind of RNase activity. Mol. Microbiol. **7:**875–882.
30. **Stolt, P., and W. Zillig.** 1993. Structure specific ds/ss-RNase activity in the extreme halophile *Halobacterium salinarium*. Nucleic Acids Res. **21:**5595–5599.
31. **Walsby, A. E.** 1994. Gas vesicles. Microbiol. Rev. **58:**94–144.
32. **Walsby, A. E., and P. K. Hayes.** 1989. Gas vesicle proteins. Biochem. J. **264:**313–322.
33. **Zamenhof, P. J., and M. Villarejo.** 1972. Construction and properties of *Escherichia coli* strains exhibiting alpha-complementation of β-galactosidase fragments in vivo. J. Bacteriol. **110:**171–178.